# Influence of Stator/Rotor Pole Combination on Electromagnetic Performance in All/Alternate Poles Wound Partitioned Stator Doubly Salient Permanent Magnet Machines

Z. Z. Wu [1], Z. Q. Zhu [1*]

[1] Department of Electronic and Electrical Engineering, University of Sheffield, Sheffield S1 3JD, U.K.
[*] z.q.zhu@sheffield.ac.uk

**Abstract:** In this paper, the influence of stator/rotor pole combinations on electromagnetic performance in partitioned stator (PS) doubly salient (DS) permanent magnet (PM) (DSPM) (PS-DSPM) machines is investigated, in terms of open-circuit flux-linkage, back-EMF, cogging torque, on-load torque characteristics. Analytical deduction shows that by modifying the all poles wound winding to alternate poles wound winding in the 12/11- and 12/13 stator/rotor pole PS-DSPM machines, the fundamental distribution factor and hence the fundamental winding factor can be enhanced, resulting higher torque density. Consequently, among the 12-stator-pole all and alternate poles wound PS-DSPM machines, the 10- and 11-rotor-pole machines exhibit the highest torque density, respectively. However, the 12/10- and 12/14-pole alternate poles wound PS-DSPM machines suffer from higher phase back-EMF even harmonics, resulting larger torque ripple. The 12/10- and 12/11-pole all and alternate poles wound prototypes are built and tested to verify the FE analysis.

Key words: All poles wound, alternate poles wound, doubly salient, partitioned stator, permanent magnet, stator/rotor pole combination.

## 1. Introduction

Stator-permanent magnet (PM) (stator-PM) machines have drawn wide attention in the last decades, due to the robust and simple rotor as well as better thermal dissipation capability than the rotor-PM machines [1]-[3]. Different from rotor-PM machines in which PMs are placed in the rotor [4]-[7], in stator-PM machines both armature windings and PMs are accommodated in the stator, leaving the rotor simple and robust. According to the PM positions, stator-PM machines can be classified to three main types, *i.e.* doubly salient (DS) PM (DSPM) machine having yoke inserted PMs [8]-[15], switched flux (SF) PM (SFPM) machines having tooth inserted PMs [16]-[18], and flux reversal (FR) PM (FRPM) machines having tooth surfaced PMs [19]-[22]. As pointed out in [1] and [2], SFPM and FRPM machines can exhibit higher torque density than DSPM machine due to more PM usage.

For improving the torque density in DSPM machines, PMs are separated from armature windings in the original stator and placed in the machine inner space to enhance the total area of them, forming partitioned stator (PS) DSPM (PS-DSPM) machine [23]. For the conventional DSPM-I machine [8]-[14] in which PM pole number is equal to the stator pole number per phase, the torque density can be enlarged by 8.49% in the corresponding PS-DSPM-I machine [23]. However, the conventional DSPM-I machine

analyzed in [8]-[14] suffers from unbalanced magnetic circuit for three-phase armature windings and hence larger torque ripple, which can be relieved in the recently proposed DSPM-II machine [15]. In the DSPM-II machine, PM pole number is equal to the stator pole number. However, this new type DSPM-II machine itself has even 5.97% smaller torque density than the conventional DSPM-I machine, although 154.98% higher PM volume is used. For this new type DSPM-II machine, torque density can be improved by 207% in the corresponding PS-DSPM-II machine. Compared with PS-DSPM-I machine, PS-DSPM-II machine has 166.08% higher torque density. Also, PS-DSPM-I machine suffers from unbalanced magnetic circuit and hence asymmetric phase back-EMF and 99.05% torque ripple which is defined as the peak to peak value to the average torque. However, this unbalanced magnetic circuit can be relieved in the PS-DSPM-II machine and the torque ripple is 84.57% smaller than the PS-DSPM-I machine, i.e. 15.28%.

Although the PS-DSPM-II machine can exhibit much higher torque density than the conventional DSPM machines, only the 12/10 stator/rotor pole all poles wound PS-DSPM-II machine is analyzed in [23], of which the torque ripple is still high caused by the large cogging torque due to the high greatest common divisor between Ns and Nr [7]. In this paper, different stator/rotor pole combinations, i.e. 12/10, 12/11, 12/13, and 12/14 will be adopted in the all and alternate poles wound PS-DSPM-II machines to evaluate the electromagnetic performance. To avoid confusing, it is noting that all the PS-DSPM machine and the DSPM machine mentioned in the following are referred to PS-DSPM-II machine and the DSPM-II machine, e.g. 12/10-pole all and alternate poles wound PS-DSPM machines shown in Fig. 1(a) and Fig. 1(b), respectively.

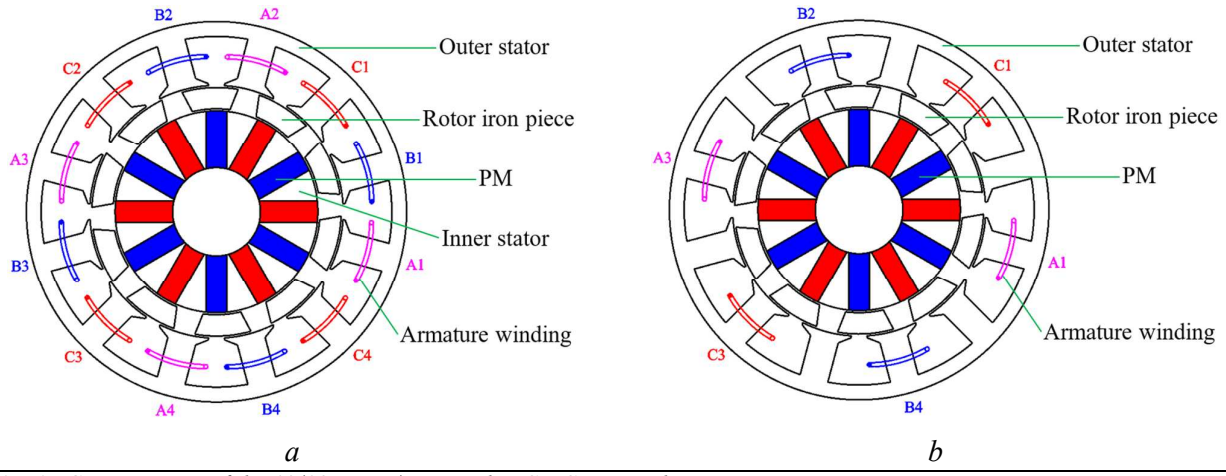


***Fig. 1.*** *Cross-section of the 12/10 stator/rotor-pole PS-DSPM machine*
a All poles wound
b Alternate poles wound

This paper is organized as follows. In section II, winding factors including both pitch factor and

distribution factor of the all/alternate poles wound PS-DSPM machines having different stator/rotor pole combinations are analytically derived. In section III, electromagnetic performance of the 12/10-, 12/11-, 12/13- and 12/14-pole all and alternate poles wound PS-DSPM machines is comparatively analyzed by finite element (FE) analysis. In section IV, 12/10- and 12/11-pole prototype machines with both all and alternate poles wound windings are built and tested to verify the FE predicted results, followed by conclusions in section V.

## 2. Feasible Stator/Rotor Pole Number Combinations

### *2.1. Fundamental Winding Factor*

Since PS-DSPM machine has non-overlapping concentrated coils, the nth pitch factor $k_{pn}$ can be given as,

$$k_{pn} = \cos\left[n\pi\left(\frac{N_r}{N_s} - 1\right)\right] \tag{1}$$

where $N_r$ and $N_s$ are the rotor and stator pole number, respectively.

As shown in (1), when $n$ is an even number, $k_{pn}$ is not zero which means the coil back-EMF suffers from even harmonics due to the even air-gap field harmonics caused by the static PMs and modulation effect of the salient rotor [28]-[31]. Therefore, in the PS-DSPM machine, the coil number per phase $N_c$ is always designed as an even number to possibly eliminate the even harmonics by appropriately selecting stator/rotor pole combination $N_s/N_r$. The coil number each phase $N_c$ in the all and alternate poles wound PS-DSPM machines can be expressed respectively as,

$$N_c = \frac{N_s}{m} \tag{2}$$

and

$$N_c = \frac{N_s}{2m} \tag{3}$$

Moreover, as shown apparently in (1), to achieve a higher fundamental pitch factor $k_{p1}$ in PS-DSPM machines, a smaller difference between $N_r$ and $N_s$ is preferred, i.e.

$$N_r = N_s \pm 1 \tag{4}$$

As $N_s$ is always an even number for $p_{PM}$-pole-pair PMs, $N_r$ will be an odd number if the combination of $N_s$ and $N_r$ is selected based on (4) and hence the rotor will suffer from the unbalanced magnetic force (UMF). Consequently, $N_s/N_r$ is also alternatively designed as [23],

$$N_r = N_s \pm 2 \tag{5}$$

In 3-phase 12-stator-pole all and alternate poles wound PS-DSPM machines, $N_r$=10, 11, 13 and 14 will be adopted in the following analysis. The coil back-EMF phasors of the analyzed 8 machines are

shown in Fig. 2, in which coil back-EMF phasor $m$' ($m$=1,2,3…12) means the opposite phasor of $m$. According to the coil back-EMF phasors shown in Fig. 2, the fundamental distribution factor $k_{d1}$ can be calculated as listed in Table 1, together with $k_{p1}$ from (1) and fundamental winding factor $k_{w1}$ is calculated by,

$$k_{w1} = k_{p1}k_{d1} \tag{6}$$

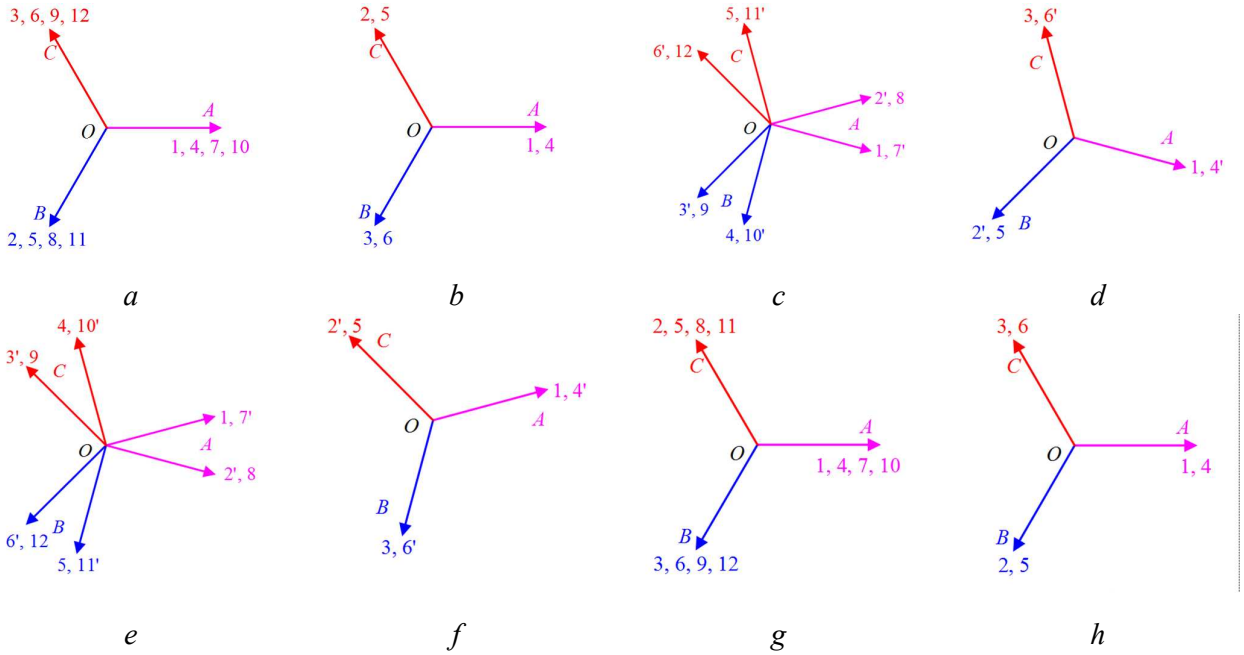


***Fig. 2.*** *Coil back-EMF phasors of the 12-stator-pole all/alternate poles wound PS-DSPM machines with 10-, 11-, 13- and 14-rotor-pole rotors*
a 10-pole all poles wound
b 10-pole alternate poles wound
c 11-pole all poles wound
d 11-pole alternate poles wound
e 13-pole all poles wound
f 13-pole alternate poles wound
g 14-pole all poles wound
h 14-pole alternate poles wound

**Table 1** Fundamental pitch factors, distribution factors and winding factors of 3-phase 12-stator-pole PS-DSPM machines

| $N_r$ | 10 | | 11 | | 13 | | 14 | |
|---|---|---|---|---|---|---|---|---|
| Winding | All | Alt | All | Alt | All | Alt | All | Alt |
| $k_{p1}$ | 0.866 | 0.866 | 0.966 | 0.966 | 0.966 | 0.966 | 0.866 | 0.866 |
| $k_{d1}$ | 1 | 1 | 0.966 | 1 | 0.966 | 1 | 1 | 1 |
| $k_{w1}$ | 0.866 | 0.866 | 0.933 | 0.966 | 0.933 | 0.966 | 0.866 | 0.866 |

As listed in Table 1, by modifying the winding type from all poles wound to alternate poles wound,

fundamental distribution factor $k_{d1}$ can be enhanced from 0.966 to 1 in the 12/11- and 12/13-pole machines, whilst in the 12/10- and 12/14-pole machines they are the same as the all poles wound counterparts. The enhancement of the fundamental distribution factor $k_{d1}$ in the 12/11- and 12/13-pole having alternate poles wound machines implies that they may produce higher torque density than their all poles wound counterparts, which will be shown later.

### *2.2. Cancellation of Coil Back-EMF Even Harmonics*

As mentioned before, coil back-EMF suffers from even harmonics in PS-DSPM machines. In this sub-section, the cancellation of coil back-EMF even harmonics is investigated as follows.

In the 12-stator-pole all poles wound PS-DSPM machines with 10-, 11-, 13- and 14-rotor-pole rotors, the coil $A_i$ ($i$=1, 2, 3, 4) back-EMF $e_{Ai}(t)$ can be expressed as,

$$e_{Ai}(t) = \sum_{k=1}^{\infty} E_k \sin(kN_r\Omega_r t + \theta_{ik}) \tag{7}$$

where $E_k$ is the coil $k^{th}$ back-EMF harmonic amplitude. $\theta_{ik}$ is the coil $A_i$ back-EMF $k^{th}$ harmonic initial phase. $\Omega_r$ is the rotor speed in unit of rad/s.

As shown in (7), whether the coil back-EMF even harmonics can be cancelled or not is depended on the difference between $\theta_{ik}$ of the coils forming a phase winding, $\Delta\theta_{ik}$, which can be given by,

$$\Delta\theta_{ik} = \theta_{ik} - \theta_{1k} = \frac{2N_r D_{1i} k\pi}{N_s} + \theta_{ad1i} \tag{8}$$

where $D_{1i}$ is the slot number distance between coils $A_1$ and $A_i$. $\theta_{ad1i}$ is the additional phase difference due to the polarities of the coil $A_i$ and its corresponding PM. They can be synthesised in Tables 2 and 3, respectively.

**Table 2** Slot number distance $D_{1i}$ between coils $A_1$ and $A_i$ in 3-phase 12-stator-pole all poles wound PS-DSPM machines

| $N_r$ | 10 | 11 | 13 | 14 |
|---|---|---|---|---|
| $D_{11}$ | 0 | 0 | 0 | 0 |
| $D_{12}$ | 3 | 1 | 1 | 3 |
| $D_{13}$ | 6 | 6 | 6 | 6 |
| $D_{14}$ | 9 | 7 | 7 | 9 |

**Table 3** Additional phase difference $\theta_{ad1i}$ of coil $A_i$ in 3-phase 12-stator-pole all poles wound PS-DSPM machines

| $N_r$ | 10 | 11 | 13 | 14 |
|---|---|---|---|---|
| $\theta_{ad11}$ | 0 | 0 | 0 | 0 |
| $\theta_{ad12}$ | $\pi$ | 0 | 0 | $\pi$ |

| | | | | |
|---|---|---|---|---|
| $\theta_{ad13}$ | 0 | $\pi$ | $\pi$ | 0 |
| $\theta_{ad14}$ | $\pi$ | $\pi$ | $\pi$ | $\pi$ |

Based on (8), Tables 2 and 3, $\Delta\theta_{ik}$ can be listed in Table 4. As shown in Table 4, in the 12/10- and 12/14-pole all poles wound machines, when $k$ is an even number, coil back-EMF even harmonics will be cancelled in coils A1 and A2 due to a π phase difference, as well as A3 and A4. When the machine winding is changed from all poles wound to alternate poles wound, only coils A1 and A3 are left for the phase A winding. The same phase between $\theta_{1k}$ and $\theta_{3k}$ indicates that the coil back-EMF even harmonics cannot be cancelled but doubled in the 12/10- and 12/14-pole all poles wound machines. This analysis can also be adopted to the coil DC flux-linkage ($k$=0).

**Table 4** $\Delta\theta_{1k}$ of coils $A_1$ and $A_i$ in 3-phase 12-stator-pole all poles wound PS-DSPM machines

| $N_r$ | 10 | 11 | 13 | 14 |
|---|---|---|---|---|
| $\Delta\theta_{1k}$ | 0 | 0 | 0 | 0 |
| $\Delta\theta_{2k}$ | $5k\pi+\pi$ | $11k\pi/6$ | $13k\pi/6$ | $7k\pi+\pi$ |
| $\Delta\theta_{3k}$ | $10k\pi$ | $11k\pi+\pi$ | $13k\pi+\pi$ | $14k\pi$ |
| $\Delta\theta_{4k}$ | $15k\pi+\pi$ | $5k\pi/6+\pi$ | $7k\pi/6+\pi$ | $21k\pi+\pi$ |

However, as shown in Table 4, in the 12/11- and 12/13-poles all poles wound PS-DSPM machines, when $k$ is an even number, coil back-EMF even harmonics will be cancelled in coils A1 and A3 due to a π phase difference, as well as A2 and A4. Moreover, coil back-EMF even harmonics can still be cancelled in the 12/11- and 12/13-poles alternate poles wound machines, in which only coils A1 and A3 are left.

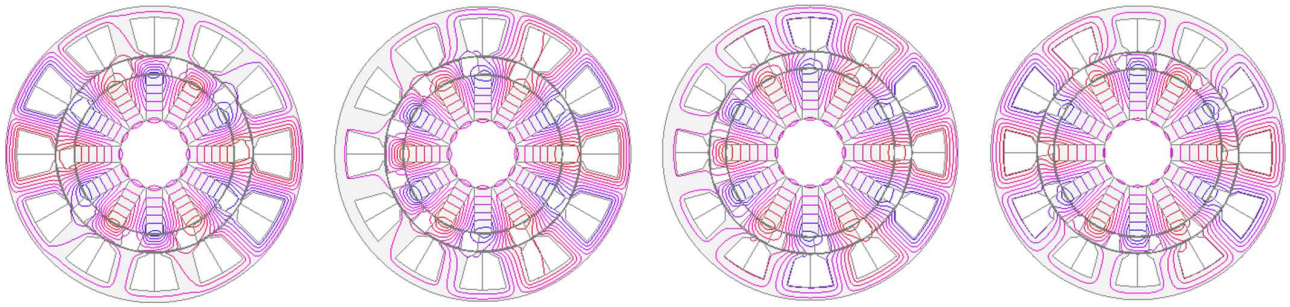

*a* *b* *c* *d*

***Fig. 3.*** *Open-circuit flux distributions of the 12-stator-pole all poles wound PS-DSPM machines at d-axis rotor position*
a 10-pole
b 11-pole
c 13-pole
d 14-pole

### *2.3. D-Axis Rotor Position*

As a synchronous machine, it is worth showing the d-axis rotor position at which the phase A winding flux-linkage achieves the maximum value. As shown in Table 4, when $k$=1, all the 4 coils forming phase A winding in 12/10- and 12/14-pole all poles wound PS-DSPM machines have the same fundamental phase. Therefore, the d-axis rotor positions can be shown as Fig. 3(a) and Fig. 3(b) for 12/10- and 12/14-pole all and alternate poles wound PS-DSPM machines, at which the rotor iron piece is aligned to the $A_1$ tooth.

When $k$=1, coils $A_1$ and $A_3$ have the same fundamental phase, which is 11π/6 and 13π/6 electric rad different from that of coils $A_2$ and $A_4$ for the 12/11- and 12/13-poles all poles wound PS-DSPM machines. For achieving a higher distribution factor, coils $A_2$ and $A_3$ are oppositely connected with $A_1$ and $A_4$ in series, as shown in Fig. 2(c) and Fig. 2(e). Therefore, as shown in Fig. 3(b) and Fig. 3(c), the rotor iron piece is π/12 electric rad advance before or lag behind the A1 tooth in the 12/11- and 12/13-pole all poles wound PS-DSPM machines at the d-axis rotor position, respectively. However, in the 12/11- and 12/13-pole alternate poles wound PS-DSPM machines, the rotor iron piece is still aligned to the $A_1$ tooth at the $d$-axis rotor position, as shown in Fig. 4(a) and Fig. 4(b), respectively. It is worth noting that in the PS-DSPM machines, the relationship between rotor position in unit of electric and mechanical rad can be given by,

$$\theta_e = N_r \theta_m \tag{9}$$

where $\theta_e$ and $\theta_m$ are rotor position in unit of electric and mechanical rad, respectively.

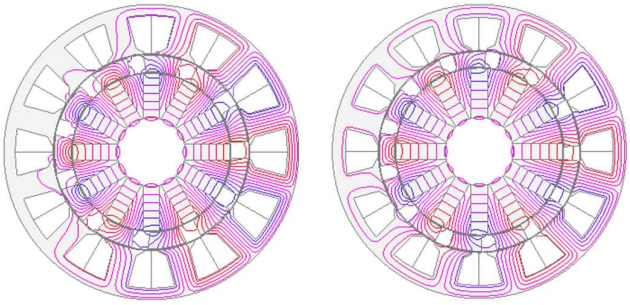

*a* *b*

***Fig. 4.*** *Open-circuit flux distributions in 12-stator-pole all poles wound PS-DSPM machines at d-axis rotor position*
a 11-pole
b 13-pole

The open-circuit flux distributions of the 12-stator-pole all poles wound PS-DSPM machines at *d*-axis rotor position are shown in Fig. 3. Fig. 4(a) and Fig. 4(b) show the open-circuit flux distributions of the 12/11- and 12/13-pole alternate poles wound PS-DSPM machines at *d*-axis rotor position, respectively. The 12/10- and 12/14-pole alternate poles wound PS-DSPM machines have the same open-circuit flux

distributions as their all poles wound counterparts as the same *d*-axis rotor position, respectively. As shown in Fig. 3 and Fig. 4, coil flux-linkage is unipolar in PS-DSPM machines due to the certain flux path direction to each coil. The coil flux-linkage DC components can be cancelled in all the analyzed machines except the 12/10- and 12/14-pole alternate poles wound PS-DSPM machines, as the same $\theta_{10}$ and $\theta_{30}$ shown in Table 4.

The design parameters of the 12-stator-pole all poles wound PS-DSPM machines having 10-, 11-, 13- and 14-rotor-pole rotors are shown in Table 5. In Table 5, parameters from $L_s$ to $T_{PM}$ are fixed for all these 4 machines, whilst those from $R_{osy}$ to $\theta_{ri}$ are obtained from the optimization with 20W copper loss and 0.5 slot packing factor for the highest average electromagnetic torque, under brushless AC (BLAC) operation mode and zero *d*-axis current control, i.e. $i_d$=0. The design parameters in Table 5 can be referred in the linear illustration shown in Fig. 5. The design parameters of the alternate poles wound machines are exactly the same with their all poles wound counterparts, respectively.

**Table 5** Design parameters of 12-stator-pole PS-DSPM machines with 10-, 11-, 13- and 14-rotor-pole rotors

| Parameters | Unit | 12/10 | 12/11 | 12/13 | 12/14 |
|---|---|---|---|---|---|
| Rotor iron piece number, $N_r$ | - | 10 | 11 | 13 | 14 |
| Stack length, $L_s$ | mm | 25 | | | |
| Outer stator outer radius, $R_{oso}$ | mm | 45 | | | |
| Inner stator inner radius, $R_{isi}$ | mm | 10.4 | | | |
| Outer air-gap width, $g_o$ | mm | 0.5 | | | |
| Inner air-gap width, $g_i$ | mm | 0.5 | | | |
| Top length of outer stator tip, $l_{ott}$ | mm | 0.5 | | | |
| Bottom length of outer stator tip, $l_{otb}$ | mm | 2 | | | |
| PM thickness, $T_{PM}$ | mm | 5 | | | |
| Outer stator yoke radius, $R_{osy}$ | mm | 41.5 | 41.5 | 41 | 41 |
| Outer stator inner radius, $R_{osi}$ | mm | 30 | 30 | 31 | 31 |
| Rotor inner edge radius, $R_{ri}$ | mm | 24.5 | 24.5 | 26 | 26 |
| Outer stator tooth arc, $\theta_{ost}$ | ° | 13 | 14 | 14 | 14 |
| Outer stator tip arc, $\theta_{ot}$ | ° | 5 | 4 | 4 | 3 |
| Rotor outer edge arc, $\theta_{ro}$ | ° | 26 | 23 | 19 | 17 |
| Rotor inner edge arc, $\theta_{ri}$ | ° | 21 | 21 | 19 | 20 |

This article has been accepted for publication in a future issue of this journal, but has not been fully edited.
Content may change prior to final publication in an issue of the journal. To cite the paper please use the doi provided on the Digital Library page.

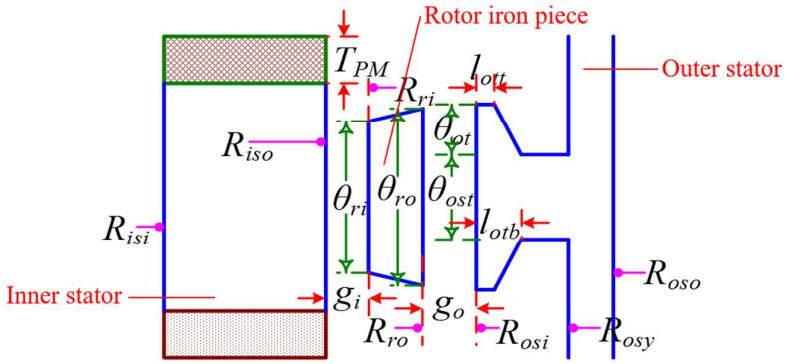


***Fig. 5.*** *Linear illustration of PS-DSPM machines*

## 3. Machines Electromagnetic Performance

In the section, electromagnetic performance of the 12-stator-pole all and alternate poles wound PS-DSPM machines having 10-, 11-, 13- and 14-rotor pole rotors are comparatively analyzed by FE, including open-circuit flux-linkage and back-EMF, torque characteristics, and UMF, as shown as follows.

### *3.1 Open-Circuit Electromagnetic Performance*

As shown in Fig. 6, there is no phase flux-linkage even harmonics nor DC component in the analyzed 12-stator-pole all poles wound PS-DSPM machine, due to the cancellation effect analyzed before, together with the 12/10-pole DSPM all poles wound machine. This is also suitable for the 12/11- and 12/13-pole alternate poles wound PS-DSPM machines. However, the 12/10- and 12/14-pole alternate poles wound PS-DSPM machines and the 12/10-pole alternate poles wound DSPM machines suffer from phase flux-linkage even harmonics and DC component, as predicted before. In Fig. 6, $N_p$ is the number of phase turns, which is 72 for all the analyzed 10 machines. Therefore, the coil number turns $N_c$=18 and $N_c$=36 in the all and alternate poles wound machines, respectively. The design parameters of the 12/10-pole DSPM machine are given in [23].

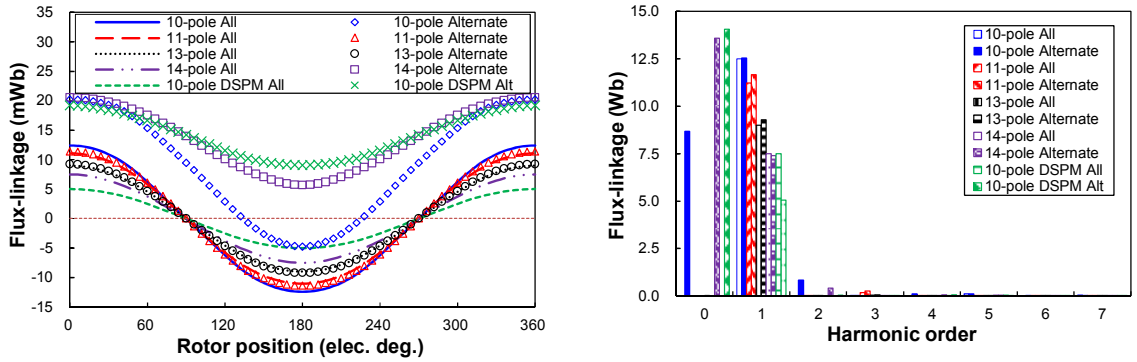


*a* *b*

***Fig. 6.*** *Phase flux-linkages of 12-stator-pole all and alternate poles wound PS-DSPM machines, $N_p$=72*
a Waveforms
b Spectra

As for the open-circuit phase back-EMF, the 12/10- and 12/14-pole alternate poles wound PS-DSPM machines suffer from phase back-EMF even harmonics again, as shown in Fig. 7, as well as the 12/10-pole alternate poles wound DSPM machine. When compared with the all poles wound 12/11 and 12/13-pole PS-DSPM machines, the phase fundamental back-EMF can be enhanced in the alternate poles wound counterparts, respectively, as shown in Fig. 7 and Table 4. This is due to the enhancement of fundamental distribution factor $k_{d1}$ and hence the fundamental winding factor $k_{w1}$ as analyzed before. However, it is similar for the 12/10- and 12/14-pole PS-DSPM machines and the 12/10-pole DSPM machines as they have similar $k_{w1}$. Among the analyzed all poles wound PS-DSPM machines, the 10-pole one has the highest phase fundamental back-EMF. However, the 11-pole one has the largest phase fundamental back-EMF among the alternate poles wound machines, which is even higher than the 10-pole all poles wound machine. Moreover, all the analyzed PS-DSPM machines have much higher phase fundamental back-EMF than the 12/10-pole DSPM machine, due to the enhancement of PM area.

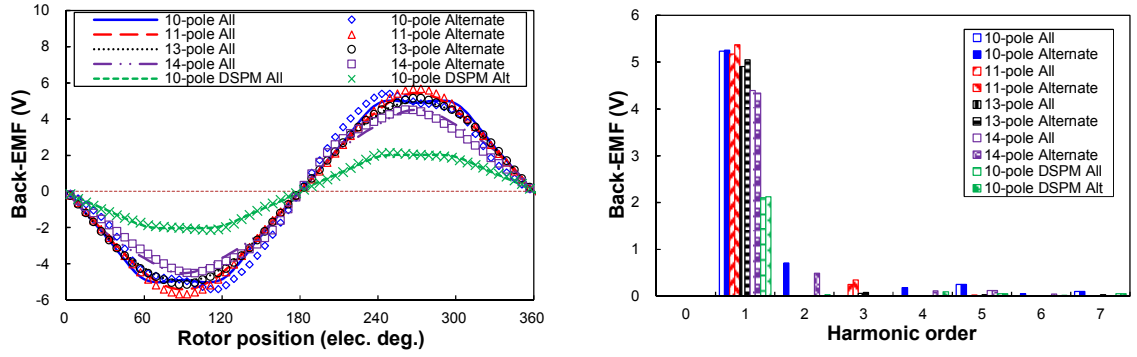


*a* *b*

***Fig. 7.*** *Phase back-EMFs of 12-stator-pole all and alternate poles wound PS-DSPM machines, $N_p$=72 @400rpm*

a Waveforms
b Spectra

**Table 6** Phase fundamental back-EMF $E_1$ @400rpm of 12-stator-pole PS-DSPM machines and 12/10-pole DSPM machine

| Machine | 10-pole PS-DSPM | | 11-pole PS-DSPM | | 13-pole PS-DSPM | | 14-pole PS-DSPM | | 12/10-pole DSPM | |
|---|---|---|---|---|---|---|---|---|---|---|
| Winding | All | Alt | All | Alt | All | Alt | All | Alt | All | Alt |
| $E_1$ (V) | 5.24 | 5.26 | 5.17 | 5.37 | 4.90 | 5.05 | 4.39 | 4.34 | 2.10 | 2.12 |

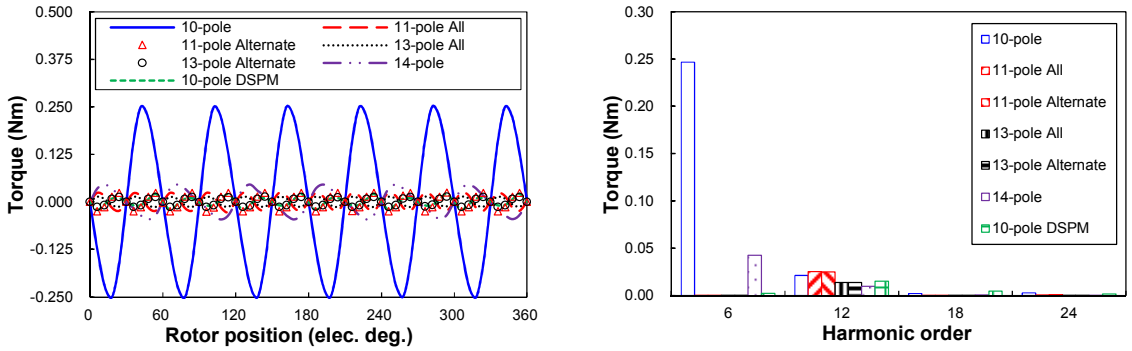


*a* *b*

***Fig. 8.*** *Cogging torques of 12-stator-pole all and alternate poles wound PS-DSPM machines*
a Waveforms
b Spectra

Another important open-circuit characteristic for PM machine is the cogging torque, which is caused by the interaction between slots and PMs [7]. As shown in Fig. 8, the 12/10- and 12/14-pole PS-DSPM machines suffer from higher cogging than the 11- and 13-pole counterparts, due to the larger greatest common divisor between $N_s$ and $N_r$ [7]. For the cogging torque cycles per electric period $N_{cog}$, it can be synthesized as,

$$N_{cog} = \frac{LCM(N_s, N_r)}{N_r} \tag{10}$$

where *LCM* is the least common multiple.

The formula shown in (10) can be evidenced by Fig. 8(b). $N_{cog}$=6 in the 12/10- and 12/14-pole PS-DSPM machines and the 12/10-pole DSPM machine, whilst $N_{cog}$=12 in the 12/11- and 12/13-pole PS-DSPM machines. The cogging torque values are listed in Table 7 as $T_{cog}$, which is defined as the peak to peak value.

### *3.2 On-load Electromagnetic Torque*

As shown in Fig. 9 and Table 7, the on-load average electromagnetic torque $T_{avg}$ decreases with rotor pole number $N_r$ in the 12-stator-pole all poles wound PS-DSPM machines. However, among the 12-stator-

pole alternate poles wound PS-DSPM machines, the 12/11-pole one exhibits the highest torque density, which is even slightly higher than the 12/10-pole all poles wound PS-DSPM machine. This trend is similar to that of the phase fundamental back-EMF shown in Fig. 7 and Table 6, due to the $i_d$=0 control. As shown in Fig. 10, since the similar *d*- and *q*-axis reluctances and hence inductances, the reluctance torque is negligible in all these analyzed 10 machines. Therefore, the $i_d$=0 control is applied to all the analyzed machines. More importantly, the PS-DSPM machines have 131.47% higher torque density higher than the 12/10-pole DSPM machines, as the enhancement of the PM and armature windings area. However, the average torque per PM volume is only 30.03% larger, due to the 60.37% higher PM volume in the PS-DSPM machines. The torque ripple $T_r$ of the 12/10- and 12/14-pole alternate poles wound PS-DSPM machines and the 12/10-pole alternate poles wound DSPM machines is much higher than other machines, due to the phase back-EMF even harmonics, as shown in Fig. 9 and Table 7. The torque ripple $T_r$ is defined as

$$T_r = \frac{T_{max} - T_{min}}{T_{avg}} * 100\% \quad (11)$$

where $T_{max}$ and $T_{min}$ are the maximum and minimum electromagnetic torques, respectively.

The enhancement of the torque density in the whole copper loss range in the PS-DSPM machines is compared with the DSPM machine in Fig. 11. Again, the torque density falls with rotor pole number in the 12-stator-pole all poles wound PS-DSPM machines, whilst the 12/11-pole alternate poles wound PS-DSPM machine exhibits the largest torque density in the whole copper loss range. More importantly, due to the enhancement of fundamental distribution factor kd1 and hence the fundamental winding factor kw1 in the 12/11- and 12/13-pole alternate poles wound PS-DSPM machines, these two machines have 2.46% and 2.03% higher torque densities than their alternate poles wound counterparts, respectively.

**Table 7** Torque characteristics of 12-stator-pole PS-DSPM machines and 12/10-pole DSPM machine

| Machine | 10-pole PS-DSPM | | 11-pole PS-DSPM | | 13-pole PS-DSPM | | 14-pole PS-DSPM | | 12/10-pole DSPM | |
|---|---|---|---|---|---|---|---|---|---|---|
| Winding | All | Alt | All | Alt | All | Winding | All | Alt | All | Alt |
| $T_{cog}$ (Nm) | 0.50 | 0.50 | 0.05 | 0.05 | 0.03 | 0.03 | 0.09 | 0.09 | 0.04 | 0.04 |
| $T_{max}$ (Nm) | 3.70 | 4.10 | 3.43 | 3.53 | 3.03 | 3.10 | 2.84 | 3.05 | 1.20 | 1.28 |
| $T_{min}$ (Nm) | 3.18 | 2.93 | 3.35 | 3.43 | 2.98 | 3.01 | 2.62 | 2.20 | 1.08 | 1.04 |
| $T_{avg}$ (Nm) | **3.46** | **3.35** | **3.39** | **3.48** | **3.00** | **3.07** | **2.73** | **2.62** | **1.13** | **1.13** |
| $T_r$ (%) | 15.02 | 34.98 | 2.30 | 3.03 | 1.52 | 2.81 | 8.14 | 32.57 | 10.74 | 21.03 |
| $V_{PM}$ (cm$^3$) | 20.49 | 20.49 | 20.49 | 20.49 | 22.74 | 22.74 | 22.74 | 22.74 | 12.77 | 12.77 |
| $T_{avg}/V_{PM}$ (Nm/cm$^3$) | 0.17 | 0.16 | 0.17 | 0.17 | 0.13 | 0.13 | 0.12 | 0.12 | 0.09 | 0.09 |

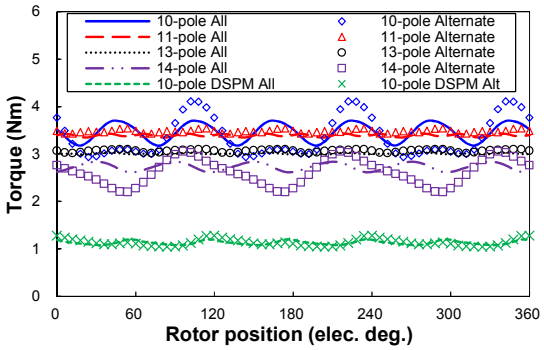


***Fig. 9.*** *On-load electromagnetic torque waveforms of 12-stator-pole all and alternate poles wound PS-DSPM machines ($p_{cu}$=20W, $i_d$=0)*

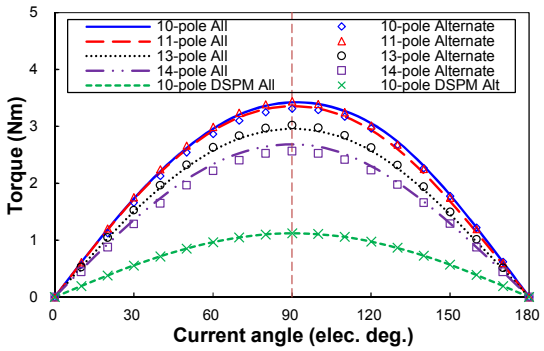


***Fig. 10.*** *Average electromagnetic torque versus current angle of 12-stator-pole all and alternate poles wound PS-DSPM machines ($p_{cu}$=20W, $i_d$=0)*

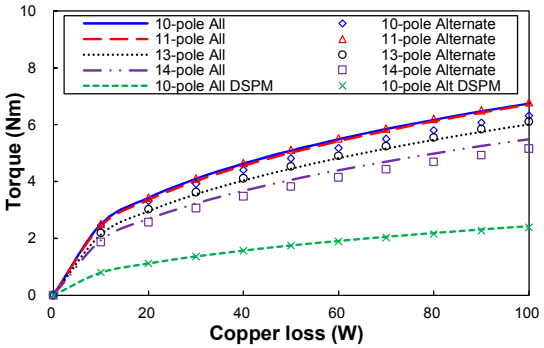


***Fig. 11.*** *Average electromagnetic torque versus copper loss of 12-stator-pole all and alternate poles wound PS-DSPM machines ($p_{cu}$=20W, $i_d$=0)*

### *3.3 Unbalanced Magnetic Force*

In the foregoing analysis, FE results show that the torque density can be enhanced in 12/11- and 12/13-pole PS-DSPM machines by modifying the all poles wound winding type to alternate poles wound. However, the 12/11- and 12/13-pole PS-DSPM machines suffer from the UMF due to the odd rotor pole number. As shown in Fig. 12, both 12/13-pole all and alternate poles wound PS-DSPM machines suffer

from higher open-circuit UMF than their 12/11-pole counterparts, respectively, as well as the on-load UMF. For the 12/13-pole PS-DSPM machines having all and alternate poles wound windings, the on-load UMFs are similar, which are also similar to the open-circuit one. However, the 12/11-pole alternate poles wound PS-DSPM machine has slightly smaller on-load UMF than its all poles wound counterpart, both of which are smaller than the open-circuit one.

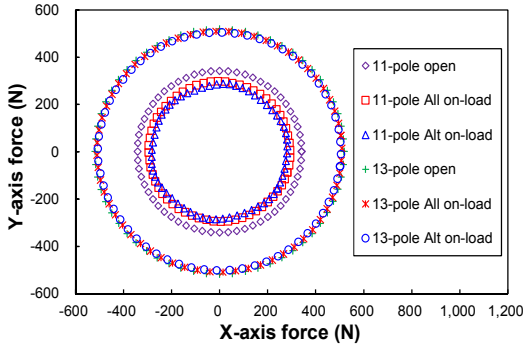


***Fig. 12.*** *Open-circuit and on-load UMFs of 12/11- and 12/13-pole all and alternate poles wound PS-DSPM machines ($p_{cu}$=20W, $i_d$=0)*

## 4. Experimental Validation

In the foregoing analysis, FE results show that the 12/10-pole and 12/11-pole machines have the highest torque density among the all and alternate poles wound PS-DSPM machines, respectively. Phase back-EMF and static torque of the 12/10-pole all poles wound PS-DSPM prototype machine is reported in [23]. In this section, both 12/10- and 12/11-pole all and alternate poles wound PS-DSPM machines are built and tested to validate the FE predicted phase back-EMFs and static torques. Fig. 13 shows the photos of the machine components. As shown in Fig. 13(a), all the 12 armature coils are open for different coil connections for 12/10- and 12/11-pole PS-DSPM machines with all and alternate poles wound. The dimensional parameters are shown in Table 8. It should be noted that $T_b$=0.5mm flux bridges are introduced in the rotor iron pieces to easy manufacturing, as shown in Fig. 13(d).

As shown in Fig. 14 to Fig. 16, both the measured and predicted phase back-EMF and static torque of the prototypes can be verified by the 2D FE predicted results, although the measured values are slightly smaller due to end-effect. In the measurement of static torques, the relationship between A-, B- and C-phase currents $I_A$, $I_B$ and $I_C$ are governed by,

$$-0.5I_A = I_B = I_C \tag{12}$$

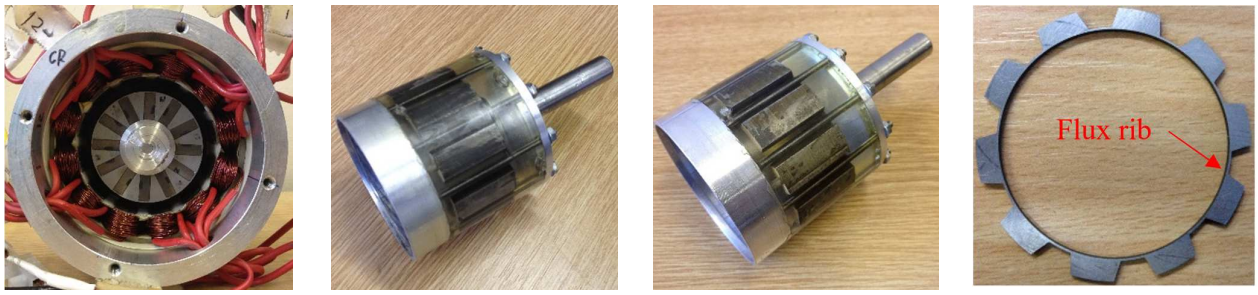


*a* *b* *c* *d*

***Fig. 13.*** *Photos of 12/10- and 12/11-pole PS-DSPM prototype machines*
a Partitioned stator
b 10-pole cup rotor
c 11-pole cup rotor
d 10-pole rotor lamination

**Table 8** Dimensional parameters of 12/10- and 12/11-pole PS-DSPM prototype machines

| Parameters | 10-pole | 11-pole | Parameters | 10-pole | 11-pole |
|---|---|---|---|---|---|
| $L_s$ (mm) | 25 | | $g_o$ (mm) | 0.5 | |
| $R_{oso}$ (mm) | 45 | | $g_i$ (mm) | 0.5 | |
| $R_{osy}$ (mm) | 42 | | $\theta_{ost}$ (°) | 8.12 | |
| $R_{osi}$ (mm) | 31.75 | | $\theta_{osy}$ (°) | 6.14 | |
| $R_{ro}$ (mm) | 31.25 | | $\theta_{ot}$ (°) | 4.94 | |
| $R_{ri}$ (mm) | 26.25 | | $l_{ott}$ (mm) | 1 | |
| $R_{iso}$ (mm) | 25.75 | | $l_{otb}$ (mm) | 3 | |
| $R_{isy}$ (mm) | 21.75 | | $\theta_{ro}$ (°) | 18 | 20 |
| $R_{isi}$ (mm) | 10.4 | | $\theta_{ri}$ (°) | 24 | 22.7 |
| $T_{PM}$ (mm) | 5 | | $\theta_{PM}$ (°) | 30 | |
| $T_b$ (mm) | 0.5 | | $N_c$ | 18 | |

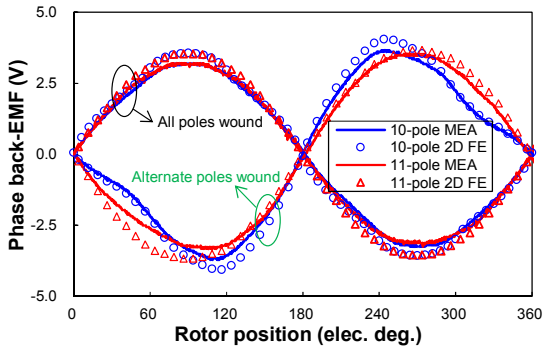


***Fig. 14.*** *Comparison of measured and 2D FE predicted phase back-EMFs at 400rpm*

Moreover, the 12/11-pole alternate poles wound PS-DSPM prototype machine has higher back-EMF and hence torque density than its all poles wound counterpart, validating the foregoing analytical and FE analysis. Also, the 12/10-pole alternate poles wound PS-DSPM prototype machine suffers from asymmetric phase back-EMF due to the even harmonics.

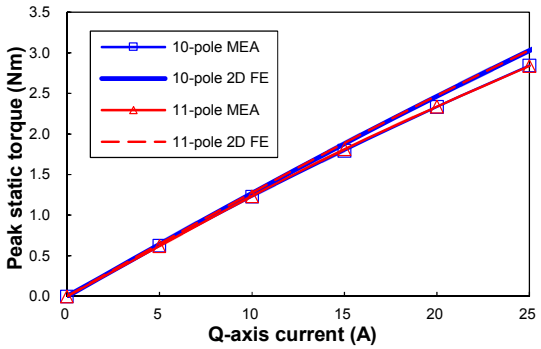


***Fig. 15.*** *Comparison of 2D FE predicted and measured peak static torques versus current in all poles wound prototype machines ($I_a$=-2$I_b$=-2$I_c$)*

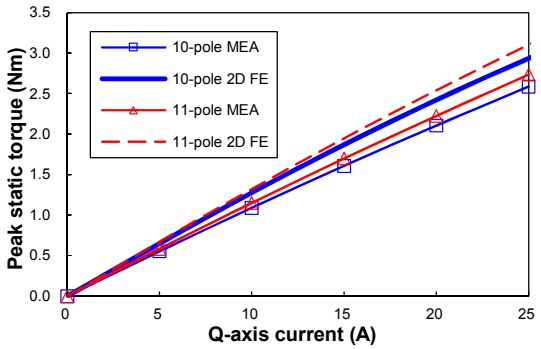


***Fig. 16.*** *Comparison of 2D FE predicted and measured peak static torques versus current in alternate poles wound prototype machines ($I_a$=-2$I_b$=-2$I_c$)*

## 5. Conclusions

In this paper, the influence of stator/rotor pole number combinations on electromagnetic performance in all and alternate poles wound PS-DSPM machines is investigated. Analytical, FE and experimental results show that compared with their all poles wound counterparts, the phase fundamental back-EMF and hence torque density can be enhanced in the 12/11- and 12/13-pole alternate poles wound PS-DSPM machines, due to the improvement of fundamental distribution factor and hence the fundamental winding factor. Consequently, the 12/11-pole machine has the highest torque density among the alternate poles wound machines whilst the 12/10-pole machine exhibits the largest torque among those all poles wound machines. However, the 12/10- and 12/14-pole alternate poles wound PS-DSPM machines suffer from phase back-EMF even harmonics and hence larger torque ripple, since the coil back-EMF even harmonics cannot be cancelled each other.

## References

[1] Zhu, Z.Q., Howe, D.: 'Electrical machines and drives for electric, hybrid and fuel cell vehicles', *Proc. IEEE*, 2007, **95**, (4), pp. 746-765

[2] Cheng M., Hua W., Zhang J., *et al.*: 'Overview of stator-permanent magnet brushless machines', *IEEE Trans. Ind. Electron.*, 2011, **58**, (11), pp. 5087-5101

[3] Chau K.T., Chan, C.C., Liu, C.H.; 'Overview of permanent-magnet brushless drives for electric and hybrid electric vehicles', *IEEE Trans. Indus. Electron.*, 2008, **55**, (6), pp. 2246-2257

[4] EL-Refaie, A.M.,: 'Fractional-slot concentrated-windings synchronous permanent magnet machines: opportunities and challenges', *IEEE Trans. Ind. Electron.*, 2010, **57**, (1), pp. 107-121

[5] Cros, J., Viarouge, P.: 'Synthesis of high performance PM motors with concentrated windings', *IEEE Trans. Energy Convers.*, 2002, **17**, (2), pp. 248-253

[6] Bianchi, N., Bolognani, S., Dai Pré, M.: 'Magnetic loading of fractional-slot three-phase PM motors with non-overlapped coils', *IEEE Trans. Ind. Appl.*, 2008, **44**, (5), pp. 1513-1521

[7] Zhu, L., Jiang, S.Z., Zhu, Z.Q., *et al.*: 'Analytical methods for minimizing cogging torque in permanent-magnet machines', *IEEE Trans. Magn.*, 2009, **45**, (4), pp. 2023-2031

[8] Liao, Y., Liang, F., Lipo, T.A.: 'A novel permanent magnet motor with doubly salient structure', *IEEE Trans. Ind. Appl.*, 1995, **31**, (5), pp. 1069-1078

[9] Cheng, M., Chau, K.T., Chan, C.C., *et al.*: 'Nonlinear varying-network magnetic circuit analysis for doubly salient permanent-magnet motors', *IEEE Trans. Magn.*, 2000, **36**, (1), pp. 339-348

[10] Cheng, M., Chau, K.T., Chan, C.C.: 'Static characteristics of a new doubly salient permanent magnet motor', *IEEE Trans. Energy Convers.*, 2001, **16**, (1), pp. 20-25

[11] Sekhar Babu, A.R.C., Rajagopal, K.R.; 'FE analysis of multiphase doubly salient permanent magnet motors', *IEEE Trans. Magn.*, 2005, **41**, (10), pp. 3955-3957

[12] Fan, Y., Chau, K.T., Cheng, M.: 'A new three-phase doubly salient permanent magnet machine for wind power generation', *IEEE Trans. Ind. Appl.*, 2006, **42**, (1), pp. 53-60

[13] Zhao, W., Cheng, M., Zhu, X., *et al.*: 'Analysis of fault-tolerant performance of a doubly salient permanent-magnet motor drive using transient cosimulation method', IEEE *Trans. Ind. Electron.*, 2008, **55**, (4), pp. 1739-1748

[14] Tai, W., Tsai, M., Gaing, Z., *et al.*:'Novel stator design of double salient permanent magnet motor', *IEEE Trans. Magn.*, 2014, **50**, (4), Art. ID 8100504

[15] Wu, D., Shi, J.T., Zhu, Z.Q., *et al.*: 'Electromagnetic performance of novel synchronous machines with permanent magnets in stator yoke', *IEEE Trans. Magn.*, 2014, **50**, (9), Art. ID 8102009

[16] Zhu, Z.Q., Pang, Y., Howe, D., *et al.*:'Analysis of electromagnetic performance of switched flux switching permanent magnet machines by non-linear adaptive lumped parameter magnetic circuit model', *IEEE Trans. Magn.*, 2005, **41**, (11), pp. 4277-4287

[17] Hoang, E., Ben Ahmed, A.H., Lucidarme, J.: 'Switching flux permanent magnet polyphased synchronous machines', *Proc. Eur. Power Electron. Conf.*, Trondheim, Norway, 1997, pp. 903-908

[18] Hua, W., Cheng, M., Zhu, Z.Q., *et al.*: 'Analysis and optimization of back EMF waveform of a flux-switching permanent magnet motor', *IEEE Trans. Energy Convers.*, 2008, **23**, (3), pp. 727-733

[19] Deodhar, R.P., Andersson, S., Boldea, I., *et al.*: 'The flux-reversal machine: a new brushless doubly-salient permanent-magnet machine', *IEEE Trans. Ind. Appl.*, 1997, **33**, (4), pp. 925-934

[20] Wang, C.X., Boldea, I., Nasar, S.A.,: 'Characterization of three phase flux reversal machine as an automotive generator', *IEEE Trans. Energy Convers.*, 2001, **16**, (1), pp. 74-80

[21] More, D.S., Fernandes, B.G.,: 'Analysis of flux-reversal machine based on fictitious electrical gear', *IEEE Trans. Energy Convers.*, 2010, **25**, (4), pp. 940-947

[22] Shi, J.T., Zhu, Z.Q., Wu D., *et al.*:'Comparative study of novel synchronous machines having permanent magnets in stator poles', *Proc. of Int. Conf. on Electrical Machines* (ICEM2014), 2014, Berlin, Germany, pp. 429-435

[23] Wu, Z.Z., Zhu, Z.Q., and Shi, J.T.: 'Novel doubly salient permanent magnet machines with partitioned stator and iron pieces rotor', *IEEE Trans. Magn.*, 2015, **51**, (5), Art. ID 8105212

[24] Bianchi, N., Bolognani, S., Pre, M.D., *et al.*:'Design considerations for fractional-slot winding configurations of synchronous machines', *IEEE Trans. Ind. Appl.*, 2006, 42, (4), pp. 997-1006

[25] Bianchi, N., Pre, M.D.: 'Use of the star of slots in designing fractional-slot single-layer synchronous motors," *Proc. Inst. Electr. Eng. Electr. Power Appl.*, 2006, pp. 459-466

[26] Bianchi, N., Pre, M.D., Alberti, L., *et al.*:'*Theory and Design of Fractional-Slot PM Machines*' (Padova, Italy: CLEUP, 2007)

[27] Chen, J.T., Zhu, Z.Q.: 'Winding configurations and optimal stator and rotor pole combination of flux-switching PM brushless AC machines', *IEEE Trans. Energy Convers.*, 2010, 25, (2), pp. 293-302

[28] McFarland, J.D., Jahns, T.M., El-Refaie, A.M.; 'Analysis of the torque production mechanism for flux-switching permanent-magnet machines', *IEEE Trans. Ind. Appl.*, 2015, 51, (4), pp. 3041-3049

[29] Li, D., Qu, R., Li, J., *et al.*:'Synthesis of flux switching permanent magnet machines', *IEEE Trans. Energy Convers.*, 2016, 31, (1), pp. 106-117

[30] Shi, Y., Jian, L., Wei, J., *et al.*: 'A new perspective on the operating principle of flux-switching permanent magnet machines', *IEEE Trans. Ind. Electron.*, 2016, 63, (3), pp. 1425-1437

[31] Wu, Z.Z., Zhu, Z.Q.: 'Analysis of air-gap field modulation and magnetic gearing effects in switched flux permanent magnet machines', *IEEE Trans. on Magn.*, 2015, 51, (5), Art. ID 8105012